J. Fluid Mech. (2000), *vol.* 418, *pp.* 339–350. Printed in the United Kingdom

Drag on a sphere moving horizontally in a stratified fluid

By M. D. GREENSLADE

Department of Applied Mathematics and Theoretical Physics, University of Cambridge, Silver Street, Cambridge CB3 9EW, UK

(Received 6 September 1999 and in revised form 24 May 2000)

The steady translational motion of a sphere in a Boussinesq stratified fluid, where the motion is parallel to the stratification surfaces, is studied. A model based on existing linear gravity wave theory for large Froude numbers and on new theory for small Froude numbers is presented. The small-Froude-number theory describes wave generation and the presence of a rectangular-section attached wake whose size and shape is controlled by the size and shape of the wave generation regions. Existing laboratory data are used to evaluate the model's prediction for the drag coefficient of the sphere as a function of Froude number.

1. Introduction

The flow produced by a solid body moving steadily horizontally through a vertically density (or entropy) stratified fluid is a fundamental element of fluid dynamics. The equivalent situation of the flow of a stratified fluid, with uniform velocity at infinity, past a fixed solid body has important applications in atmospheric and oceanic dynamics, where many flows of interest are topographically generated.

To take the simplest case, we examine the motion of a rigid sphere translating steadily through an incompressible fluid uniformly stratified in density (or, equivalently, a Boussinesq fluid uniformly stratified in potential temperature). By uniform stratification we mean that the buoyancy (Brunt–Väisälä) frequency is uniform. For an incompressible fluid the buoyancy frequency, N, is related to the undisturbed density field, $\rho(z)$, by $N^2 = -(g/\rho)\mathrm{d}\rho/\mathrm{d}z$, while for a Boussinesq fluid N is related to the undisturbed potential temperature field, $\theta(z)$, by $N^2 = (g/\theta)\mathrm{d}\theta/\mathrm{d}z$; here z is the vertical (stratification) coordinate in each case.

Writing ν for the kinematic viscosity of the fluid (assumed uniform), r for the radius of the sphere, and U for the translation speed of the sphere, there are two dimensionless similarity parameters for this flow: the Reynolds number and the Froude number, defined respectively as

$$\mathscr{R} = \frac{2Ur}{\nu} \quad \text{and} \quad \mathscr{F} = \frac{U}{Nr}.$$

In the following it is assumed that the Reynolds number is large, which is certainly the case in relevant geophysical applications. Then for a large range of Reynolds numbers and Froude numbers the motion of the fluid is complex and difficult to describe comprehensively. We therefore focus attention on just one observable aspect of the flow: the drag force exerted by the fluid on the sphere.

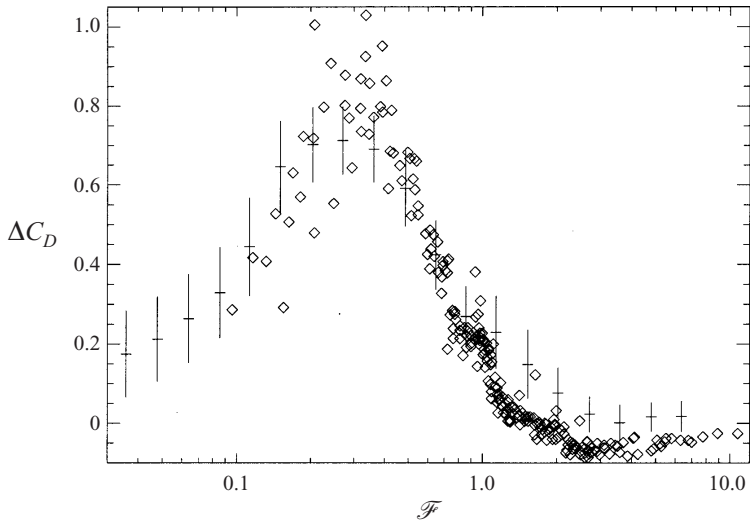

FIGURE 1. Laboratory measurements of ΔC_D versus $\mathscr{F}$. The scatter bars (19 values of $\mathscr{F}$) are from Mason (1977), and represent mean measurements and standard errors. The diamond symbols (245 data points) are from Lofquist & Purtell (1984).

Let D be the magnitude of the drag force on the sphere. In non-dimensional terms this can be expressed in the standard way as a drag coefficient

$$C_D(\mathscr{R},\mathscr{F}) = \frac{D}{\frac{1}{2}\rho_0 U^2 \pi r^2},$$

where ρ_0 is the undisturbed fluid density at the level of the centre of the sphere. In order to examine the effects of stratification only we define the modified drag coefficient

$$\Delta C_D(\mathscr{R},\mathscr{F}) = C_D(\mathscr{R},\mathscr{F}) - C_D(\mathscr{R},\infty),$$

where $C_D(\mathscr{R},\infty)$ is the measured drag coefficient for the given value of $\mathscr{R}$, but in the unstratified case ($\mathscr{F} = \infty$). For sufficiently large $\mathscr{R}$, ΔC_D is found to be nearly independent of $\mathscr{R}$ (e.g. the experimental data of Lofquist & Purtell 1984 used in the following), suggesting that ΔC_D is a measure of pressure drag only, with the effects of any frictional drag subtracted. The aim of this study is to explain the observed dependence of ΔC_D on $\mathscr{F}$ in this large-$\mathscr{R}$ regime.

Figure 1 shows a plot of ΔC_D versus $\mathscr{F}$ for a composite of two sets of data from laboratory experiments: Mason (1977) and Lofquist & Purtell (1984). The scatter shown in Mason's data is partly accounted for by oscillations of the measured drag coefficients with time in each of his experimental runs. Lofquist & Purtell, on the other hand, chose to time-average their measurements. The predominant feature of both sets of data is unimodal dependence of ΔC_D on $\mathscr{F}$. The maximum value of ΔC_D is in the approximate range $(0.6, 1.1)$, at a value of $\mathscr{F}$ in the approximate range $(0.2, 0.5)$. For $\mathscr{F} \gtrsim 0.5$, each set of data collapses onto a narrow band (small scatter), showing values of ΔC_D which decrease with increasing $\mathscr{F}$, at least up to $\mathscr{F} \approx 3$; for larger values of $\mathscr{F}$, ΔC_D is approximately constant. A discrepancy between the two sets of data is apparent for $\mathscr{F} \gtrsim 1$, with the Mason data giving consistently larger values of ΔC_D than the Lofquist & Purtell data. The Lofquist & Purtell data actually show negative values of ΔC_D for $\mathscr{F} \gtrsim 2$. The latter feature is possibly related to the

modification of the wake shape by stratification (compared with unstratified flow, $\mathscr{F} = \infty$), as suggested by Castro, Snyder & Baines (1990). However, its absence from the Mason data prevents us from drawing any conclusions. For $\mathscr{F} \lesssim 0.2$, both sets of data show a larger scatter, reflecting the extreme difficulty of taking measurements in this range, where laboratory towing speeds and absolute drag values are very small. However, there is sufficient consistency within each set of data, and between the two sets, to give a clear indication of the increase of ΔC_D with increasing $\mathscr{F}$ in this range.

A more recent set of related laboratory data is provided by Vosper *et al.* (1999). However, the differences between these data and those of Mason (1977) and Lofquist & Purtell (1984) prevent a direct comparison. These differences may be due to the fact that Vosper *et al.*'s experimental set-up comprises a surface-mounted hemisphere, rather than a fully submerged sphere. Furthermore, Vosper *et al.*'s Froude number range is limited to $\mathscr{F} \geqslant 0.2$, so that the trend of ΔC_D increasing with increasing $\mathscr{F}$, as shown by the data of Mason and Lofquist & Purtell, is not evident.

Another interesting comparison is with the numerical simulations of Hanazaki (1988). Hanazaki compares his numerical model output directly with the drag values measured by Mason (1977) and Lofquist & Purtell (1984). The agreement for larger Froude numbers is good, but there is a quantitative discrepancy for $\mathscr{F} \lesssim 0.5$. This is probably attributable to Hanazaki's relatively small model Reynolds number: $\mathscr{R} = 200$.

Our aim in this paper is to explain the most fundamental features of the experimental data by constructing a model which shows a similar unimodal dependence of ΔC_D on $\mathscr{F}$. Our study proceeds as follows. In § 2 we describe component quantitative theoretical models for the physical features in the flow responsible for the drag. The small-$\mathscr{F}$ theory, as applied to this problem, and formulae (2.7), (2.8), (2.9) resulting from it are new. In § 3 we compare the theories with the laboratory data. This comparison is also new, even for the existing large-$\mathscr{F}$ theory. We also discuss the intermediate-$\mathscr{F}$ range, where neither the large-$\mathscr{F}$ theory, nor the small-$\mathscr{F}$ theory are expected to be strictly valid. We describe the behaviour of the flow in this range qualitatively. In § 4 we summarize our results.

2. Analysis

There are two physical processes producing the pressure drag on the sphere. The first is the generation of internal gravity waves, associated with the vertical fluid motions near the sphere. The second is the separation of the viscous boundary layer from the surface of the sphere, leading to an attached wake behind the sphere; this is an inescapable feature of high-Reynolds-number flow past a bluff body. In the laboratory experiments of Mason (1977) and Lofquist & Purtell (1984), there was time-variation of the measured drag values in each experimental run, although these authors effectively presented only their time-averaged results (with the scatter bars of Mason's data points giving some indication of the time-variation). The analysis described here assumes (statistically) steady flow. It can therefore be interpreted as applying to the time-averaged experimental data.

2.1. *Large-$\mathscr{F}$ theory*

For large $\mathscr{F}$ a theoretical prediction of the wave field and wave drag has been given by Gorodtsov & Teodorovich (1982). Their analysis is based on modelling the rigid sphere as a surface distribution of mass sources and sinks. The approximation they use is that the distribution is assumed to be the same as it would be in the homogeneous

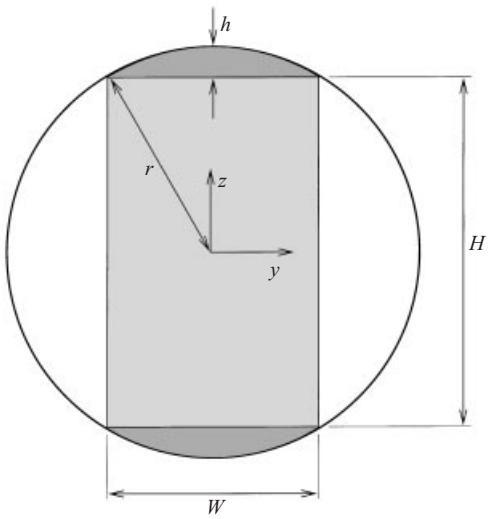

FIGURE 2. Aft view of the sphere showing the geometry of the wave generation regions (dark shading) and the wake (light shading) for small $\mathscr{F}$.

(unstratified) fluid case. This approach then gives a linear theory prediction for the wave field in terms of convolutions of the mass source/sink distribution with a Green function. The result is, for the wave drag on the sphere,

$$D = \tfrac{9}{16}\rho_0 N^2 \pi^2 r^4 \mathscr{F} \int_1^\infty \frac{J_{3/2}(\xi/\mathscr{F})^2}{\xi^3(\xi^2-1)^{1/2}}\mathrm{d}\xi,$$

or

$$C_D = \frac{D}{\frac{1}{2}\rho_0 U^2 \pi r^2} = \frac{9\pi}{8}\mathscr{F}^{-1}\int_1^\infty \frac{J_{3/2}(\xi/\mathscr{F})^2}{\xi^3(\xi^2-1)^{1/2}}\mathrm{d}\xi, \tag{2.1}$$

where J is the Bessel function of the first kind. While it is a simple enough matter to integrate this numerically, we can also adopt Gorodtsov & Teodorovich's asymptotic simplification for large $\mathscr{F}$:

$$D \sim \tfrac{1}{8}\rho_0 N^2 \pi r^4 \mathscr{F}^{-2}(\ln \mathscr{F} + \tfrac{7}{4} - \gamma) \quad \text{for } \mathscr{F} \gg 1,$$

or

$$C_D \sim \tfrac{1}{4}\mathscr{F}^{-4}(\ln \mathscr{F} + \tfrac{7}{4} - \gamma) \quad \text{for } \mathscr{F} \gg 1, \tag{2.2}$$

where γ is Euler's constant ($= 0.577$). If we assume that the drag due to the attached wake varies only weakly with $\mathscr{F}$ for $\mathscr{F} \gg 1$ we can use these formulae for C_D as an estimate for ΔC_D.

2.2. *Small-$\mathscr{F}$ theory*

The theory here is a development of that presented in Greenslade (1994) and Hunt *et al.* (1997). Refer to figure 2.

Drazin (1961) showed that, in the limit $\mathscr{F} \to 0$, the fluid motion is purely horizontal. Correspondingly, the isopycnal surfaces (isentropic surfaces in the Boussinesq case) are horizontal and, in the frame of reference in which the sphere is stationary, the fluid passes around either side of the sphere. Greenslade (1994) showed that for small but finite $\mathscr{F}$ there are regions near the top and bottom of the sphere for which this is not the case. The structure of the flow can best be summarized by considering the

geometry of the isopycnal surfaces. For arbitrary finite $\mathscr{F}$ we can define a pair of isopycnal surfaces which are in contact with the top and bottom of the sphere and which are at elevations $z = \pm z_s$ far from the sphere (taking $z = 0$ at the centre of the sphere). In the unstratified limit $\mathscr{F} \to \infty$, $z_s = 0$. In the opposite limit $\mathscr{F} \to 0$, Drazin's theory predicts $z_s = r$. For small but finite $\mathscr{F}$, Greenslade's theory predicts $z_s = (1 - A\mathscr{F})r$, where A is an order-unity positive constant independent of $\mathscr{F}$. The two streamlines which lie in the vertical plane of symmetry of the flow and which are embedded in these isopycnal surfaces (one in each surface) are known as the dividing streamlines, and in the following we refer to the isopycnal surfaces as the dividing streamsurfaces. Laboratory measurements of z_s by Snyder *et al.* (1985) and Vosper *et al.* (1999) for bodies which are locally spherical at their top and bottom agree with Greenslade's theoretical prediction and give values of A close to 1. It is geometrically clear that the isopycnal surfaces in between the dividing streamsurfaces are all pierced by the sphere, so that the flow in these surfaces is around the sphere, as in the Drazin solution. The remaining isopycnal surfaces are all simply connected (not pierced by the sphere), and the flow in these surfaces can reasonably be described as going above or below the sphere. The geometry of the flow is illustrated well by the numerical simulations of Hanazaki (1988).

The theory of Greenslade (1994) pays further attention to the small regions of flow adjacent to the top and bottom of the sphere where fluid is passing above and below the sphere, and suggests that gravity waves are generated there. Wave generation in or near these regions, with associated downstream propagation, is certainly seen in all laboratory experiments conducted with spheres and surface-mounted hemispheres (most recently Vosper *et al.* 1999; Chomaz, Bonneton & Hopfinger 1993; Lin *et al.* 1992). We can model this wave generation by applying the linear, hydrostatic model of Smith (1980) to a body in the form of a spherical cap of height $h = A\mathscr{F}r$ and spherical radius r mounted on a horizontal plane (which serves as the simplest estimated position of the dividing streamsurface). The base diameter of the spherical cap is $W = 2^{3/2}A^{1/2}\mathscr{F}^{1/2}(1 - \frac{1}{2}A\mathscr{F})^{1/2}r \approx 2^{3/2}A^{1/2}\mathscr{F}^{1/2}r$ for $\mathscr{F} \ll 1$. Introducing horizontal coordinates x and y in the frame of reference in which the sphere is stationary, and such that (x, y, z) has origin at the centre of the sphere, we write $z = \pm(z_s + f(x, y))$ for the equations of the estimated dividing streamsurfaces. So the function f describes the spherical cap shape, has value h at $(x, y) = (0, 0)$ and has value 0 for all points with $(x^2 + y^2)^{1/2} \geqslant W/2$. Then the model of Smith gives, for the distribution of excess pressure along the estimated dividing streamsurfaces,

$$p'(x, y) = \rho_0 UN \int_{-\infty}^{\infty} \mathrm{d}k \int_{-\infty}^{\infty} \mathrm{d}l \frac{\mathrm{i}k}{(k^2 + l^2)^{1/2}} \hat{f}(k, l) \exp\left[\mathrm{i}(kx + ly)\right], \tag{2.3}$$

where the integrand contains the Fourier transform

$$\hat{f}(k, l) = \frac{1}{(2\pi)^2} \int_{-\infty}^{\infty} \mathrm{d}x \int_{-\infty}^{\infty} \mathrm{d}y f(x, y) \exp\left[-\mathrm{i}(kx + ly)\right].$$

We can now perform some order-of-magnitude estimates. First note that $\hat{f}(0, 0) \propto hW^2$, where here and in the following the proportionality symbol stands for 'equals a constant times', where the constant is order unity, positive and independent of $\mathscr{F}$. Furthermore, $f(x, y)$ is a function of $(x^2 + y^2)^{1/2}$ only, and has a lengthscale $(x^2 + y^2)^{1/2} \propto W$. So $\hat{f}(k, l)$ is a function of $(k^2 + l^2)^{1/2}$ only, and has a 'lengthscale' $(k^2 + l^2)^{1/2} \propto W^{-1}$. Hence the maximum excess pressure on the estimated dividing

streamsurface (actually on the spherical cap portion) is

$$|p'|_{\max} \propto \rho_0 UN \times W^{-2} \times hW^2 = \rho_0 UNh \propto \rho_0 U^2 \tag{2.4}$$

for $\mathscr{F} \ll 1$. The form of the integrand in (2.3) indicates that the excess pressure on the estimated dividing streamsurface is in phase with the slope of the surface in the x-direction, with high pressure on the upstream side and low pressure on the downstream side. This gives a net drag associated with the wave generation as

$$D^{\text{waves}} = \int_{-\infty}^{\infty} \mathrm{d}x \int_{-\infty}^{\infty} \mathrm{d}y\, p'(x,y) \frac{\partial f}{\partial x}(x,y) \propto \rho_0 UNh \times hW \propto \rho_0 U^{7/2} N^{-3/2} r^{1/2} \tag{2.5}$$

for $\mathscr{F} \ll 1$.

The hydrostatic assumption of Smith's theory used in the derivation above is justified by the fact that the characteristic horizontal wavelengths of the gravity waves generated are of the order of the lengthscale of the spherical cap, W, and for small $\mathscr{F}$ this is much larger than the typical downstream distance travelled by a fluid parcel in a buoyancy period, $2\pi U/N$: $W/(2\pi U/N) \propto \mathscr{F}^{-1/2} \gg 1$ for $\mathscr{F} \ll 1$. The linear assumption of Smith's theory is not strictly justifiable; in fact the theory would only be justified if the height, h, of the spherical cap were much less than U/N, but $h/(U/N) = A$, an order-unity positive constant independent of $\mathscr{F}$. However, Smith (1980) shows that the linear hydrostatic theory gives qualitatively useful results even in this regime. Furthermore, Greenslade (1994) confirms the order-of-magnitude drag estimate (2.5) using singular perturbation theory, with no linearization assumption.

The isopycnal surfaces between the dividing streamsurfaces are pierced by the sphere and, according to the Drazin and Greenslade theories, correspond to nearly horizontal (for $\mathscr{F} \ll 1$) flow around the sphere. The laboratory experiments cited above confirm that vertical streamline displacements are much smaller than the diameter of the sphere for small $\mathscr{F}$. The laboratory experiments also show that this nearly horizontal flow separates from the downstream side of the sphere, leaving an attached wake. This wake gives a contribution to the drag on the sphere distinct from that associated with wave generation at the top and bottom of the sphere. The most important factor in determining the wake drag is the separation line of the wake. Laboratory experiments by Sysoeva & Chashechkin (1988) indicate that for small $\mathscr{F}$ this wake is rectangular in cross-section immediately behind the sphere. In discussions of their own laboratory experiments Chomaz *et al.* (1992, 1993) and Lin *et al.* (1992) have questioned these observations and have reported non-rectangular wakes. More recent experimental studies by Hunt & Fernando (1999) based on flow past more general bluff body shapes give more support to the Sysoeva & Chashechkin observations, and offer a partial theoretical justification for the wake shape, developing earlier work by Hunt *et al.* (1997). We adopt the working hypothesis of a rectangular wake in the expectation that it gives a model which is accurate at leading order for moderately small $\mathscr{F}$. There is an implicit suggestion in the work of Hunt & Fernando that the wake has a step-like rather than a rectangular cross-section for very small $\mathscr{F}$, but existing laboratory experiments on spheres and surface-mounted hemispheres have probably not been carried out at sufficiently small $\mathscr{F}$ to verify this (J. C. R. Hunt, personal communication). We follow Hunt *et al.* in making the model assumption that the dimensions of the wake are determined by the size and position of the wave generation regions, as shown in figure 2. So the width of the wake in the y-direction is W, and its height in the z-direction is $H = 2(1 - A\mathscr{F})r$. Note that this model implies that the position of the separation line at the sides of the wake is, through its dependence on W, dependent on $\mathscr{F}$.

By any standard wake model, we may assume as the most basic result that the maximum pressure difference between the fore and aft parts of the sphere over the rectangular wake area is of order $\rho_0 U^2$ (note that this is of the same order as the maximum excess pressure in the wave generation region estimated by Smith's linear theory, (2.4)). Hence we can estimate the drag due to the wake as the product of this maximum pressure difference and the cross-sectional area of the wake:

$$D^{\text{wake}} \propto \rho_0 U^2 \times HW \propto \rho_0 U^2 r^2 \mathscr{F}^{1/2}(1 - A\mathscr{F})(1 - \tfrac{1}{2}A\mathscr{F})^{1/2}$$
$$\propto \rho_0 U^2 r^2 \mathscr{F}^{1/2}(1 - \tfrac{5}{4}A\mathscr{F}) \tag{2.6}$$

for $\mathscr{F} \ll 1$, where for consistency in the following we retain two terms in the Taylor expansion for small $\mathscr{F}$.

Combining the expressions (2.5), (2.6), we get, for the drag coefficient for the whole sphere,

$$C_D = C_D^{\text{waves}} + C_D^{\text{wake}},$$

where

$$C_D^{\text{waves}} = \frac{D^{\text{waves}}}{\frac{1}{2}\rho_0 U^2 \pi r^2} = B\mathscr{F}^{3/2} \tag{2.7}$$

and

$$C_D^{\text{wake}} = \frac{D^{\text{wake}}}{\frac{1}{2}\rho_0 U^2 \pi r^2} = C\mathscr{F}^{1/2}(1 - \tfrac{5}{4}A\mathscr{F}), \tag{2.8}$$

where B and C are order-unity positive constants. Then the total modified drag coefficient is, at first three orders in $\mathscr{F}$,

$$\Delta C_D = -C_D(\mathscr{R}, \infty) + a\mathscr{F}^{1/2} + b\mathscr{F}^{3/2}, \tag{2.9}$$

where

$$a = C, \qquad b = B - \tfrac{5}{4}AC,$$

and, as above, $C_D(\mathscr{R}, \infty)$ represents the drag coefficient in the limit of infinitely large $\mathscr{F}$ (unstratified flow). The laboratory data of Mason (1977) provide us with the estimate $C_D(\mathscr{R}, \infty) = 0.52$ (a comparable value can be inferred from the unaveraged graphical data of Lofquist & Purtell 1984) which we use in the following. The parameters a and b are chosen below by statistical fitting to the laboratory data. Note that, according to this theory, C_D^{waves} is a monotonic increasing function of $\mathscr{F}$ (from (2.7)), and the ratio

$$\frac{C_D^{\text{wake}}}{C_D^{\text{waves}}} = \frac{C}{B}(\mathscr{F}^{-1} - \tfrac{5}{4}A) \tag{2.10}$$

is a monotonic decreasing function of $\mathscr{F}$.

3. Evaluation of theories

3.1. *Large-$\mathscr{F}$ theory*

Figure 3 shows a comparison of Gorodtsov & Teodorovich's (1982) formulae (2.1), (2.2) with the laboratory data. The theory clearly captures the observed decrease of ΔC_D with increasing $\mathscr{F}$ for $\mathscr{F} \gtrsim 0.5$. The agreement between the theory and the experimental data is good for $\mathscr{F} \gtrsim 1$, at least to the level of the unexplained differences between the two sets of data. The formula (2.1) gives $C_D > 0$ for all $\mathscr{F}$, so the negative values of ΔC_D observed by Lofquist & Purtell (1984), and ascribed to the effect of stratification on the wake by Castro *et al.* (1990), are not predicted by

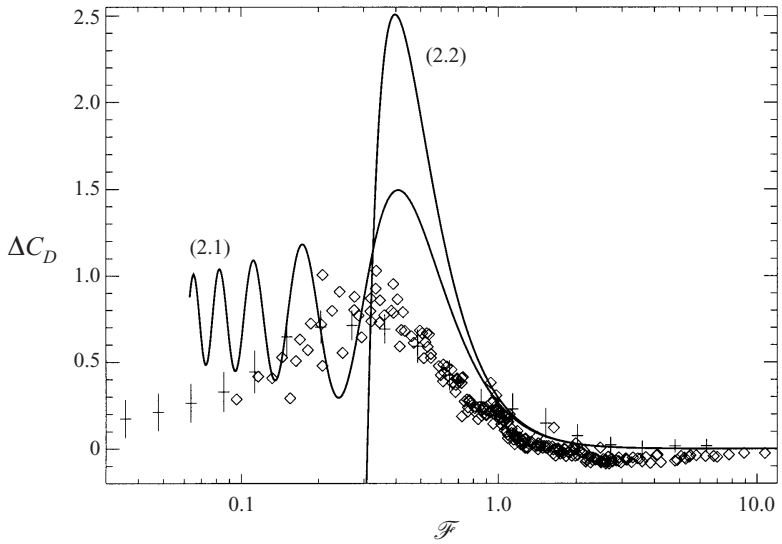

FIGURE 3. Data as in figure 1, on a stretched ordinate, with the theoretical predictions of Gorodtsov & Teodorovich (1982), equations (2.1), (2.2), superimposed (solid curves).

this theory. The agreement between the theory and the experimental data for $\mathscr{F} \lesssim 1$ is not so good. However, the theory does appear to give a reasonable estimate for the value of $\mathscr{F}$ corresponding to the maximum observed value of ΔC_D: (2.1) predicts C_D is maximized for $\mathscr{F} = 0.41$ and (2.2) predicts C_D is maximized for $\mathscr{F} = 0.40$. Both of these values are in the approximate observed range, $\mathscr{F} \in (0.2, 0.5)$, for the maximum value of ΔC_D.

3.2. *Small-$\mathscr{F}$ theory*

Figure 4 shows a plot of $\mathscr{F}^{-1/2}(\Delta C_D + C_D(\mathscr{R}, \infty))$ versus $\mathscr{F}$, with $C_D(\mathscr{R}, \infty) = 0.52$ as given by Mason (1977), for $\mathscr{F} \leqslant 1$. According to the small-$\mathscr{F}$ theory described in § 2.2, resulting in formula (2.9), we expect the laboratory data to follow a linear function in this plot. The data appear to support this hypothesis for $0.2 \lesssim \mathscr{F} \lesssim 0.8$, although there is some uncertainty associated with the large scatter in the data for $0.2 \lesssim \mathscr{F} \lesssim 0.4$. Least-squares fits of the form $\mathscr{F}^{-1/2}(\Delta C_D + C_D(\mathscr{R}, \infty)) = a + b\mathscr{F}$ to the two sets of data for $0.2 < \mathscr{F} < 0.8$ give $a = 3.33$ and $b = -3.44$ for the Mason data, and $a = 3.43$ and $b = -3.42$ for the Lofquist & Purtell (1984) data, and these are illustrated on the plot. We need to check that the values for the parameters a and b given by the least-squares fits are consistent with choices of A, B, and C which are order unity and positive. We still have a choice of one arbitrary constant. If we make the choice $A = 1$ suggested by the experimental determinations of dividing streamline heights (Snyder *et al.* 1985; Vosper *et al.* 1999) then $B = 0.73$ and $C = 3.33$ for the fit to the Mason data, and $B = 0.86$ and $C = 3.43$ for the fit to the Lofquist & Purtell data. In either case the results are consistent.

For $\mathscr{F} \gtrsim 0.8$ the data show a change in behaviour, with a distinctly smaller slope in figure 4. For $\mathscr{F} \lesssim 0.2$ there is an insignificant number of points in the data of Lofquist & Purtell (1984), and the data of Mason (1977) have a very large scatter which span the least-squares fits but do not allow us to claim agreement with the theory with any reasonable degree of confidence.

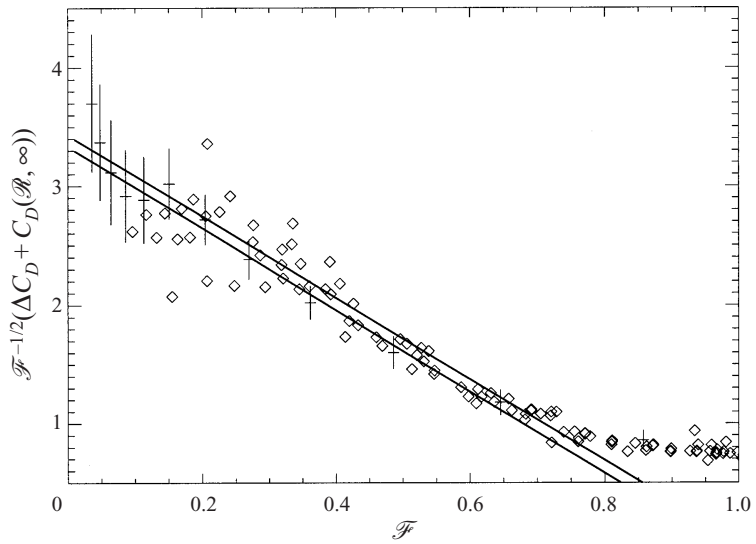

FIGURE 4. Data as in figure 1, plotted as $\mathscr{F}^{-1/2}(\Delta C_D + C_D(\mathscr{R},\infty))$ versus $\mathscr{F}$, with $C_D(\mathscr{R},\infty) = 0.52$, on a linear abscissa and only for $\mathscr{F} < 1$. Two straight lines, $a + b\mathscr{F}$ versus $\mathscr{F}$, are superimposed, with a and b chosen by least-squares fits to the two sets of data for $0.2 < \mathscr{F} < 0.8$. The lower line fits the Mason (1977) data and the upper line fits the Lofquist & Purtell (1984) data.

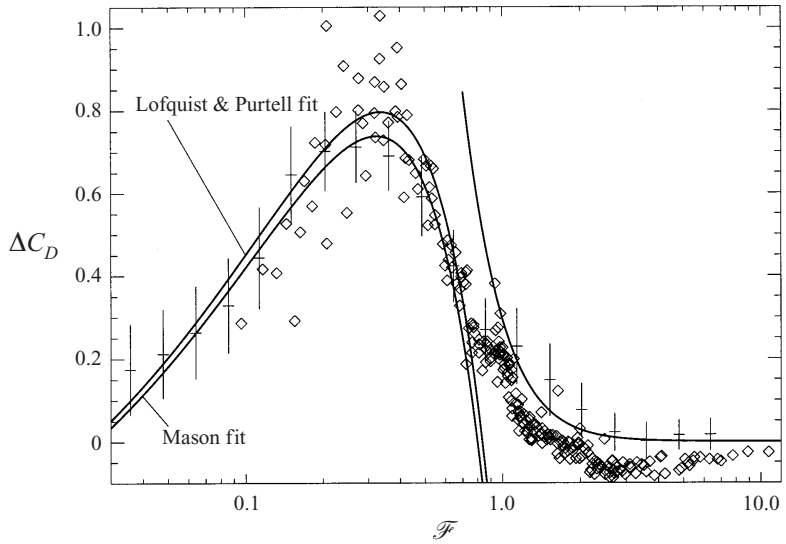

FIGURE 5. Data as in figure 1, but with the theoretical predictions (2.2) for larger $\mathscr{F}$ and (2.9) for smaller $\mathscr{F}$ superimposed (solid curves). The parameters a and b for the curves for smaller $\mathscr{F}$ are chosen by the least-squares fits shown in figure 4.

3.3. *Composite theory*

Figure 5 shows a plot of the experimental data with the model predictions (2.2) and (2.9) superimposed. The two predictions do a reasonable job of estimating the modified drag coefficient over the entire Froude number range, with the possible exception of a narrow intermediate range around $\mathscr{F} = 1$, where neither theoretical prediction is expected to be strictly valid, and where the two predictions are rather different from each other.

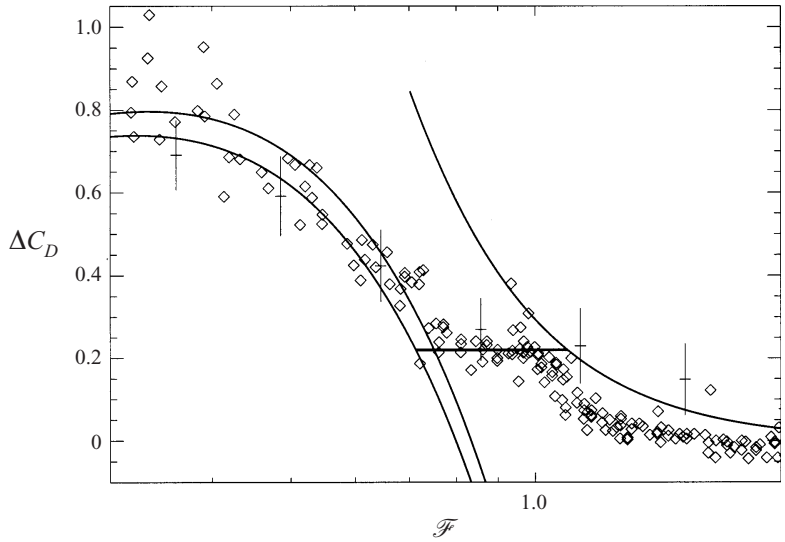

FIGURE 6. Data and theory as in figure 5, but showing only the range $\mathscr{F} \in (0.3, 2)$. The thick horizontal line is an empirical estimate of the constant value of ΔC_D in the intermediate-$\mathscr{F}$ range.

Interestingly, this narrow intermediate range around $\mathscr{F} = 1$ shows a characteristic feature in both sets of laboratory data: ΔC_D is relatively constant for $\mathscr{F} \in (0.8, 1.1)$, compared with its behaviour immediately outside this range. This is illustrated more clearly in the magnified portion of the plot shown in figure 6.We speculate that the weak dependence of ΔC_D on $\mathscr{F}$ in this range is related to wave saturation.

Consider the change in behaviour as $\mathscr{F}$ decreases from large values. For $\mathscr{F} \gg 1$ the linear wave theory of Gorodtsov & Teodorovich (1982) gives a reasonable prediction for the wave field, and hence for the drag. But general linear wave theory predicts wave overturning when $\mathscr{F}$ falls below a critical value of order unity (the precise value depends on the exact wave spectrum), say $\mathscr{F} = \mathscr{F}_1$. In reality this leads to local convective instability and subsequent nonlinear processes which constrain the maximum wave amplitude approximately to its value at $\mathscr{F} = \mathscr{F}_1$ – this is what is meant by wave saturation. So as $\mathscr{F}$ decreases below $\mathscr{F}_1$ there is no increase in the maximum wave amplitude, and so no increase in the drag. This is consistent with the data for the drag on the sphere if we take $\mathscr{F}_1 \approx 1.1$. The Gorodtsov & Teodorovich formula (2.2) gives $C_D = 0.22$ for this value of $\mathscr{F}$, and this is indicated by the thick horizontal line in figure 6.

For $\mathscr{F} \lesssim 0.8$ the small-$\mathscr{F}$ theory described in § 2.2 gives a good estimate for ΔC_D provided that we choose the two parameters a and b in (2.9) to fit the data. As $\mathscr{F}$ decreases below 0.8, the model predicts that C_D^{waves} decreases (from (2.7)) as a consequence of the waves being generated by regions of the sphere of decreasing size (frontal area); the wave field may still be locally saturated. The ratio $C_D^{\text{wake}}/C_D^{\text{waves}}$ increases rapidly with decreasing $\mathscr{F}$ (from (2.10)), so the wake drag dominates over the wave drag for most of the small-$\mathscr{F}$ range shown. According to our model the wake drag is maximized when the cross-sectional area of the wake is maximized, i.e. when the wake is square. Taking $A = 1$ as above then gives $\mathscr{F} = 1 - 2^{-1/2} = 0.29$ for the value of $\mathscr{F}$ corresponding to maximum wake drag, which is within the observed range for the maximum of ΔC_D.

4. Summary

We have constructed a model for the flow induced by a sphere moving horizontally through a vertically stratified fluid at large Reynolds number, $\mathscr{R}$. The model gives predictions for the pressure drag on the sphere, which is explained in terms of internal gravity wave generation and by the presence of an attached wake. The model predicts the dependence of each of these drag contributions on the Froude number, $\mathscr{F}$.

For large $\mathscr{F}$ our model adopts the linear wave theory of Gorodtsov & Teodorovich (1982), together with a wake whose contribution to the drag is assumed to be independent of $\mathscr{F}$. The dependence of the wave drag on $\mathscr{F}$ is described by the drag coefficient formula (2.1) or, to a sufficient degree of accuracy, by the approximate formula (2.2).

For small $\mathscr{F}$ our model is a development of the theory of Greenslade (1994) and Hunt *et al.* (1997). The wave generation is limited to narrow regions of depth $h \propto \mathscr{F} r$ and width $W \propto \mathscr{F}^{1/2} r$ (for $\mathscr{F} \ll 1$) at the top and the bottom of the sphere; the wave drag is calculated on the basis of a linear model and gives the contribution (2.7) to the total drag coefficient. The wake is rectangular in cross-section immediately behind the sphere and has depth $H = 2(r - h)$ and width W; it gives the contribution (2.8) to the total drag coefficient. The total drag coefficient is then (2.9). Importantly, the size and shape of the wake is controlled by the size and shape of the wave generation regions.

Our model reproduces the unimodal dependence of the modified drag coefficient, ΔC_D, on $\mathscr{F}$ previously observed in the laboratory experiments of Mason (1977) and Lofquist & Purtell (1984) – see figure 5. The transition from ΔC_D increasing with increasing $\mathscr{F}$ to ΔC_D decreasing with increasing $\mathscr{F}$ is apparently within the range of applicability of the small-$\mathscr{F}$ component of the model. However, the values of $\mathscr{F}$ and ΔC_D at the transition are not predicted by the model, which uses least-squares fits to the experimental data to determine two model parameters. For the smallest experimental Froude numbers ($\mathscr{F} \lesssim 0.2$) the scatter of the experimental data prevents an assessment of the model's validity. For the largest experimental Froude numbers ($\mathscr{F} \gtrsim 1$) there is insufficient agreement between the two sets of experimental data to make a quantitative assessment of the model's accuracy. The Froude number range $\mathscr{F} \in (0.8, 1.1)$ shows a transition in the experimental data; we give a speculative explanation for this in terms of wave saturation in § 3.3.

I would like to thank Dr B. Voisin for bringing the paper Gorodtsov & Teodorovich (1982) to my attention and for providing useful comments on an early draft of the paper, Professor J. C. R. Hunt for bringing the paper Hunt & Fernando (1999) to my attention and for useful discussions on the paper, and Mr J. Hampson for a useful suggestion concerning the analysis of the data.

REFERENCES

Castro, I. P., Snyder, W. H. & Baines, P. G. 1990 Obstacle drag in stratified flow. *Proc. R. Soc. Lond.* A **429**, 119–140.

Chomaz, J. M., Bonneton, P., Butet, A., Perrier, M. & Hopfinger, E. J. 1992 Froude number dependence of the flow separation line on a sphere towed in a stratified fluid. *Phys. Fluids* A **4**, 254–258.

Chomaz, J. M., Bonneton, P. & Hopfinger, E. J. 1993 The structure of the near wake of a sphere moving horizontally in a stratified fluid. *J. Fluid Mech.* **254**, 1–21.

Drazin, P. G. 1961 On the steady flow of a fluid of variable density past an obstacle. *Tellus* **13**, 239–251.

Gorodtsov, V. A. & Teodorovich, 'E. V. 1982 Study of internal waves in the case of rapid horizontal motion of cylinders and spheres. *Izv. Akad. Nauk SSSR, Mekh. Zhid. i Gaza* **17**(6), 94–100. Available in English translation in *Fluid Dyn.* **17**(6), 893–898, 1983.

Greenslade, M. D. 1994 Strongly stratified airflow over and around mountains. In *Stably Stratified Flows: Flow and Dispersion over Topography* (*Proc. 4th IMA Conf. on Stably Stratified Flows, University of Surrey, Sept. 1992*) (ed. I. P. Castro & N. J. Rockliff). Oxford University Press.

Hanazaki, H. 1988 A numerical study of three-dimensional stratified flow past a sphere. *J. Fluid Mech.* **192**, 393–419.

Hunt, J. C. R., Feng, Y., Linden, P. F., Greenslade, M. D. & Mobbs, S. D. 1997 Low Froude number stable flows past mountains. *Il Nuovo Cimento* **20C**, 261–272.

Hunt, J. C. R. & Fernando, H. J. S. 1999 Separated flow around bluff obstacles at low Froude number; vortex shedding and estimates of drag. In *Mixing and Dispersion in Stably Stratified Flows* (*Proc. 5th IMA Conf. on Stably Stratified Flows, University of Dundee, Sept. 1992*) (ed. P. A. Davies). Oxford University Press.

Lin, Q., Lindberg, W. R., Boyer, D. L. & Fernando, H. J. S. 1992 Stratified flow past a sphere. *J. Fluid Mech.* **240**, 315–354.

Lofquist, K. E. B. & Purtell, L. P. 1984 Drag on a sphere moving horizontally through a stratified liquid. *J. Fluid Mech.* **148**, 271–284.

Mason, P. J. 1977 Forces on spheres moving horizontally in a rotating stratified fluid. *Geophys. Astrophys. Fluid Dyn.* **8**, 137–154.

Smith, R. B. 1980 Linear theory of stratified hydrostatic flow past an isolated mountain. *Tellus* **32**, 348–364.

Snyder, W. H., Thompson, R. S., Eskridge, R. E., Lawson, R. E., Castro, I. P., Lee, J. T., Hunt, J. C. R. & Ogawa, Y. 1985 The structure of strongly stratified flow over hills: Dividing-streamline concept. *J. Fluid Mech.* **152**, 249–288.

Sysoeva, E. Ya. & Chashechkin, Yu. D. 1988 Spatial structure of a wake behind a sphere in a stratified liquid. *Z. Prikl. Mekh. Teckh. Fiz.* **29**(5), 59–65. Available in English translation in *J. Appl. Mech. Tech. Phys.* **29**(5), 655–660, 1988.

Vosper, S. B., Castro, I. P., Snyder, W. H. & Mobbs, S. D. 1999 Experimental studies of strongly stratified flow past three-dimensional orography. *J. Fluid Mech.* **390**, 223–249.